Selenium isotopes record extensive marine suboxia during the Great Oxidation Event

Michael A. Kipp[a,b,1], Eva E. Stüeken[a,b,c,d], Andrey Bekker[c], and Roger Buick[a,b]

[a]Department of Earth & Space Sciences and Astrobiology Program, University of Washington, Seattle, WA 98195-1310; [b]Virtual Planetary Laboratory, NASA Astrobiology Institute, Seattle, WA 98195-1310; [c]Department of Earth Sciences, University of California, Riverside, CA 92521; and [d]Department of Earth & Environmental Sciences, University of St. Andrews, St. Andrews, KY16 9AL, Scotland, United Kingdom

Edited by Mark H. Thiemens, University of California, San Diego, La Jolla, CA, and approved December 13, 2016 (received for review September 24, 2016)

It has been proposed that an "oxygen overshoot" occurred during the early Paleoproterozoic Great Oxidation Event (GOE) in association with the extreme positive carbon isotopic excursion known as the Lomagundi Event. Moreover, it has also been suggested that environmental oxygen levels then crashed to very low levels during the subsequent extremely negative Shunga–Francevillian carbon isotopic anomaly. These redox fluctuations could have profoundly influenced the course of eukaryotic evolution, as eukaryotes have several metabolic processes that are obligately aerobic. Here we investigate the magnitude of these proposed oxygen perturbations using selenium (Se) geochemistry, which is sensitive to redox transitions across suboxic conditions. We find that $\delta^{82/78}$Se values in offshore shales show a positive excursion from 2.32 Ga until 2.1 Ga (mean +1.03 ± 0.67‰). Selenium abundances and Se/TOC (total organic carbon) ratios similarly show a peak during this interval. Together these data suggest that during the GOE there was pervasive suboxia in near-shore environments, allowing nonquantitative Se reduction to drive the residual Se oxyanions isotopically heavy. This implies O_2 levels of >0.4 μM in these settings. Unlike in the late Neoproterozoic and Phanerozoic, when negative $\delta^{82/78}$Se values are observed in offshore environments, only a single formation, evidently the shallowest, shows evidence of negative $\delta^{82/78}$Se. This suggests that there was no upwelling of Se oxyanions from an oxic deep-ocean reservoir, which is consistent with previous estimates that the deep ocean remained anoxic throughout the GOE. The abrupt decline in $\delta^{82/78}$Se and Se/TOC values during the subsequent Shunga–Francevillian anomaly indicates a widespread decrease in surface oxygenation.

Paleoproterozoic | trace metals | oxygen | eukaryote evolution

The accumulation of molecular oxygen in Earth's atmosphere and ocean fundamentally restructured biogeochemical pathways, and ultimately allowed the evolution of aerobically respiring eukaryotic life. Determining the tempo of the rise of oxygen to modern levels has thus been the focus of decades of research (1, 2). The beginning of the Paleoproterozoic Era (2.5–1.6 Ga) is of particular interest, because it was the first time in Earth's history when oxygen-rich conditions prevailed in surface environments for a prolonged interval (3).

The first permanent step in the oxygenation of Earth's surface, the Great Oxidation Event (GOE), was originally identified by the disappearance of redox-sensitive detrital minerals (4, 5) and the appearance of red beds (6) around the Archean–Proterozoic boundary. More recently, the record of mass-independent fractionation of sulfur isotopes (MIF-S) in sedimentary sulfates and sulfides (7) revealed that atmospheric O_2 increased from negligible amounts to $>10^{-5}$ times present atmospheric levels (8) between 2.45 and 2.32 Ga, which is now thought to mark the onset of the GOE (9, 10).

Although its name may seem to imply a discrete upward step in the oxidation state of Earth's surface, a new view is emerging of the GOE as a dynamic interval of rising and then falling O_2 lasting until ∼2.06 Ga (3, 11). The occurrence of the largest and longest-lived positive carbon isotope excursion in the geologic record—the Lomagundi Event (LE) (12)—in the later stages of the GOE between 2.22 and 2.06 Ga, has been cited as evidence of enhanced organic carbon burial that may have allowed high levels of free oxygen to temporarily accumulate at Earth's surface at this time (13), i.e., an "oxygen overshoot" (3).

Indeed, there is mounting evidence for expansion and contraction of the marine sulfate reservoir across the LE (14–16), which is thought to reflect trends in oxidative sulfide weathering and oxygenation of the ocean as atmospheric oxygen levels rose and fell. Relative iodate abundances in carbonates also document an increase in shallow-water oxidation state near the onset of the GOE, peaking during the LE (17). Additionally, enrichments of molybdenum (Mo) and uranium (U) in organic-rich shales reflect vigorous oxidative weathering of the continents during the GOE (18, 19). Thus, a fairly consistent picture is emerging of an O_2-rich world between ∼2.3 and 2.1 Ga.

However, whereas the above proxies have indicated widespread oxygen availability in the early Paleoproterozoic, we still lack precise constraints on the extent of oxic, suboxic, and anoxic (including euxinic) habitats in the oceans at this time. This is a matter of great evolutionary importance, because the spatial and temporal transience of oxic-to-suboxic environments may have been the dominant throttle on eukaryotic evolution before the late Neoproterozoic (0.8–0.54 Ga) (20). If oxygenated habitats were indeed abundant during the GOE, it could have constituted the first time in Earth's history that geographically extensive regions of the ocean were conducive to the evolution of complex life.

Accurately probing the redox landscape of the oceans during the GOE requires a suite of proxies that function at different spatial scales. Evidence for large marine sulfate, iodate, Mo, and U reservoirs is suggestive of a global expansion of oxygenated water masses. However, these signals lack the resolution to assess

Significance

Oxygen is essential for eukaryotic life. The geologic record of early Earth contains abundant evidence of low oxygen levels, and accordingly, a lack of eukaryote fossils. The rise of oxygen to near-modern levels at the end of the Proterozoic Era is thus often cited as the trigger for the evolutionary radiation of complex life forms at this same time. Here we present selenium geochemical data that indicate an expansion of suboxic (>0.4 μM O_2) habitats in the shallow oceans between 2.32 and 2.1 Ga—more than one billion years before eukaryotes become abundant in the fossil record. These environments could have harbored the earliest stages of eukaryotic evolution, but may have been too transient for substantial diversification to occur.

Author contributions: M.A.K., E.E.S., A.B., and R.B. designed research; M.A.K. and E.E.S. performed research; M.A.K. and E.E.S. analyzed data; and M.A.K., E.E.S., A.B., and R.B. wrote the paper.

The authors declare no conflict of interest.

This article is a PNAS Direct Submission.

[1]To whom correspondence should be addressed. Email: kipp@uw.edu.

This article contains supporting information online at www.pnas.org/lookup/suppl/doi:10.1073/pnas.1615867114/-/DCSupplemental.

basinal redox gradients that could be critical for eukaryote ecology. Conversely, Fe speciation is a well-developed local redox indicator, and has been used to identify euxinia in offshore environments during the GOE (16, 21). But, because this signal records local conditions, with spatially limited data it lacks the ability to distinguish an oxygen-minimum zone in an otherwise globally oxic ocean from a globally anoxic deep ocean.

Selenium (Se) is well-suited for bridging the gaps between the aforementioned proxies, as its relatively short oceanic residence time ($\sim 10^3$ y) makes Se sensitive to basin-scale redox dynamics. Selenium is predominantly delivered to the oceans via oxidative weathering, making the marine Se reservoir scale with continental oxidative weathering rates. Additionally, Se isotopes can be fractionated by several permil during oxyanion (SeO_4^{2-}, SeO_3^{2-}, $HSeO_3^-$) reduction to elemental Se and selenide in suboxic environments, such as modern oxygen-minimum zones and suboxic pore waters. In these settings, if Se oxyanions are continuously supplied from oxygenated waters, reduction is nonquantitative and the resulting isotopic values of reduced Se compounds are typically negative (22, 23). Negative Se isotope ratios in sedimentary rocks can therefore be an indication that the sediments were deposited in an environment that was linked to a large oxic reservoir. Selenium isotopes have been used in this way to track the oxygenation of the deep ocean in the late Neoproterozoic, where fractionations down to −1.5‰ have been recorded in offshore shales that received upwelling Se oxyanions from oxic deep oceans (24). In modern anoxic basins where Se oxyanions are not continuously resupplied, Se is largely consumed by uptake into biomass without net fractionation and the reduction of Se oxyanions is quantitative (25). Isotopic values in these settings are therefore typically heavy, approaching or exceeding the composition of seawater, which is ∼+0.3‰ today (23).

We measured Se abundance and isotope ratios in organic-rich shales from seven stratigraphic units deposited in offshore environments during and after the GOE. These lithologies capture the offshore Se reservoir, which records basin-scale redox structure. Viewed together, these snapshots of individual basins at different stages of the GOE offer a glimpse of secular changes in the redox structure of the global ocean. Our results thus provide a proxy record that can test the predictions made by other redox-sensitive indicators and help resolve the spatial and temporal distribution of oxic, suboxic, and anoxic marine environments during the GOE. Specifically, these data allow us to test whether the Paleoproterozoic oxygen overshoot was at any time comparable in magnitude to the Neoproterozoic oxygenation event, and to assess the implications for the early evolution of eukaryotic life.

Materials

We analyzed 75 samples from 7 shale units deposited between 2.2 and 1.85 Ga. These data were compared with 567 published Se measurements from samples with ages spanning 3.25 Ga to the present. Samples corresponding to the early stage of the GOE come from the Rooihoogte and Timeball Hill formations of the Pretoria Group (2.32 Ga), which were analyzed by Stüeken et al. (23), and are the oldest open-marine shales deposited without an MIF-S signature. In addition, we sampled the Wewe Slate (∼2.2–2.1 Ga) and Sengoma Argillite Formation (∼2.2–2.1 Ga), which were deposited in the middle of the GOE, during the Lomagundi carbon isotope excursion. Samples straddling the end of the GOE and Lomagundi carbon isotope excursion come from the Hautes Chutes Formation of the Labrador Trough (∼2.1 Ga), the Francevillian Series of Gabon (∼2.083 Ga), the Zaonega Formation of Karelia, Russia (∼2.11–2.06 Ga), and the Union Island Group of the Slave craton (∼2.1–2.0 Ga). In addition, organic-rich shales of the Menihek Formation from the Labrador Trough (1.85 Ga), postdating the LE, were also analyzed. These samples span the latest stages of the GOE and the 200 My interval after its termination, and include the formations in which the Shunga–Francevillian negative carbon isotope anomaly was originally discovered (11).

Results

Shales deposited in offshore environments show a broad trend in Se concentrations across the GOE, with abundances increasing in the late Archean and subsequently falling through the Paleoproterozoic, with a peak between 2.32 and 2.1 Ga (max. 27.97 ppm; Fig. 1). Mean Se abundance of shales deposited between 2.32 and 2.1 Ga (6.79 ppm) is significantly higher than the mean Se abundance for shales older than 2.45 Ga (2.04 ppm; $p_{\text{one-tailed}} = 10^{-8}$) and with ages between 2.1 and 1.1 Ga (2.02 ppm; $p_{\text{one-tailed}} = 10^{-8}$). Se/TOC (total organic carbon) ratios similarly show a peak (max. 26.84 ppm/wt %) in the early stage of the GOE, but rapidly decline between 2.1 and 2.0 Ga to <<1 ppm/wt % (Figs. 1 and 2).

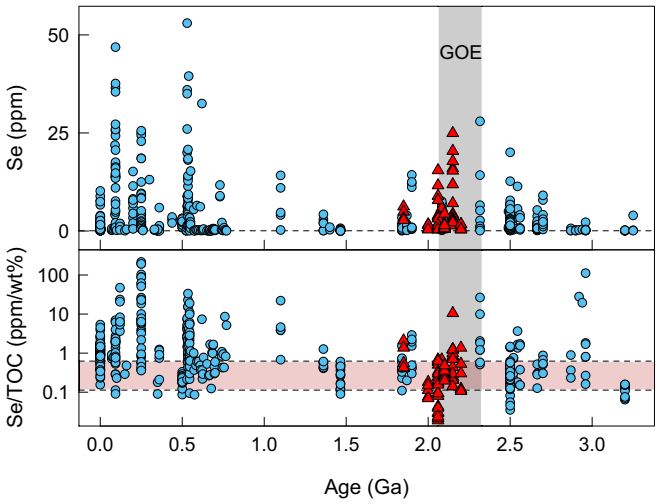

Fig. 1. Se abundance and Se/TOC (ppm/wt %) ratios in shales through geologic time (triangles, this study; circles, published data). Dotted lines represent crustal Se abundance (*Top*) and range of Se/TOC ratios in modern phytoplankton (22) (*Bottom*).

$\delta^{82/78}$Se values are consistently positive from 2.32 Ga until 2.1 Ga, and higher than in any other time in the geologic record (avg. +1.03 ± 0.67‰; Figs. 2 and 3). The mean $\delta^{82/78}$Se value for samples older than 2.45 Ga is statistically indistinguishable from that for samples dating between 2.1 and 1.1 Ga ($p_{\text{two-tailed}} = 0.11$), whereas samples with 2.32–2.1 Ga ages have significantly higher $\delta^{82/78}$Se values than both groups ($p_{\text{one-tailed}} = 10^{-10}$, 10^{-10}). Negative $\delta^{82/78}$Se values do not become prevalent until the late Neoproterozoic (24), and persist throughout the Phanerozoic (23) (Fig. 3).

Oxidative Weathering and the Marine Se Reservoir. In light of mounting evidence for elevated atmospheric oxygen levels between 2.32 and 2.06 Ga (3, 15–19), it is unsurprising that shales show an increase in Se abundance at this time (Fig. 1). Whereas Se can also be sourced to the marine environment by volcanism and hydrothermal activity, oxidative weathering is by far the dominant source on the modern Earth (∼90% of flux to oceans; volcanism ∼10%, hydrothermal input <<1%; ref. 26). Furthermore, the parallel enrichment of U (19), Mo (18), and Se in samples from the Rooihoogte and Lower Timeball Hill formations and the Sengoma Argillite Formation is most parsimoniously explained by enhanced oxidative weathering. Unlike Se, U is exclusively delivered to the oceans via oxidative mobilization, and not by volcanic or hydrothermal inputs. Additionally, Mo is not volatile and thus cannot derive from volcanic sources. Although it is not possible to definitively rule out a volcanic contribution to the sedimentary Se enrichment seen during the GOE, the vast majority of Se was likely delivered by oxidative continental weathering.

The trend in Se abundance does not correspond exactly with the inferred beginning and end of the GOE (Fig. 1). Se concentrations begin to increase in the late Archean (∼2.7 Ga), perhaps due to increasing rates of oxidative weathering in locally oxic environments on land (27). In the wake of the GOE, Se abundances remain higher than mid-Archean values until at least 1.9 Ga, and

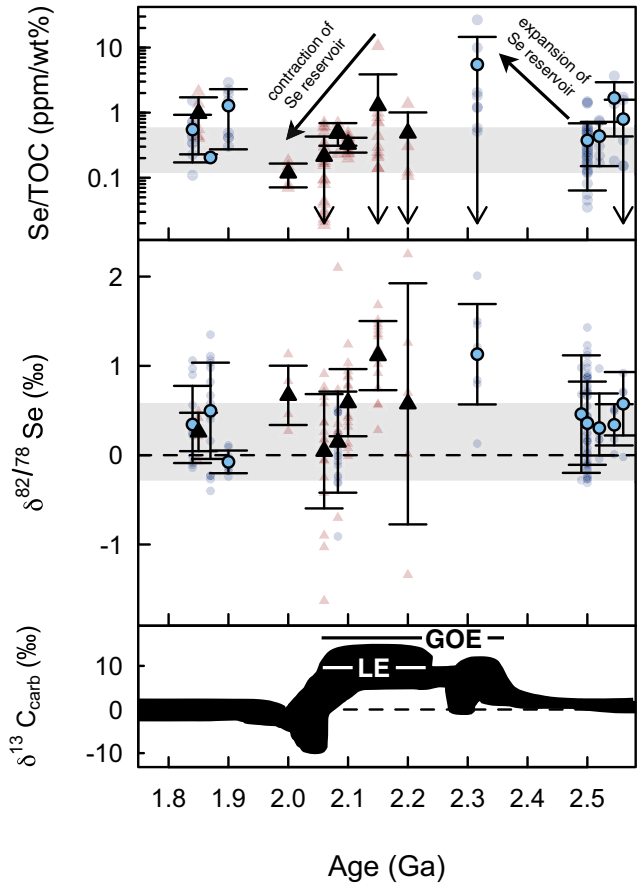

Fig. 2. Trends in Se/TOC, $\delta^{82/78}$Se, and $\delta^{13}C_{carb}$ (triangles, this study; circles, published data). Gray bands mark range of phytoplankton Se/TOC (*Top*) and crustal $\delta^{82/78}$Se (*Middle*). $\delta^{13}C_{carb}$ curve adapted from Lyons et al. (2). Solid data points are average per formation, error bars are 1σ; shadowed data points are individual samples. Note log scale in top plot.

then return to low levels in the mid-Proterozoic. This trend could suggest that atmospheric oxygen levels (and thus oxidative weathering rates) did not experience a sharp fall at the end of the GOE. However, weathering of Se-rich sediments that were deposited during the GOE and subsequently uplifted on tectonic timescales of ∼100 My could have potentially contributed to the Se enrichment seen in shales deposited after ∼2.06 Ga, leaving open the possibility that atmospheric oxygen levels did indeed decline abruptly, but the Se flux decayed slowly. In either case, it would seem that the marine Se reservoir grew larger during the GOE than at any other time before the late Neoproterozoic.

Se/TOC ratios may be a more robust indicator of Se reservoir size than Se abundance, because they account for differences in primary productivity across depositional environments. Biological incorporation of Se and subsequent settling of organic material may be the dominant mechanism of Se transport to anoxic sediments; normalizing data to organic carbon contents can thus gauge "Se excess" in the system. Like Se abundance, Se/TOC ratios steadily increase through the late Archean, and peak during the GOE at 2.32 Ga (max. 26.63 ppm/wt %). However, in contrast to the trend seen in Se abundance, Se/TOC ratios decline rapidly at the end of the GOE (Figs. 1 and 2). This decline coincides with the falling limb of the Lomagundi carbon isotope excursion, which has been argued to record a time of rapid deoxygenation (15, 16). The decreasing Se/TOC ratios therefore may suggest that the marine Se reservoir was in fact rapidly shrinking at the end of the GOE with the expansion of marine anoxia. Maximum enrichments greater than 10 ppm/wt % are not observed again for ∼1 Gy after the termination of the GOE.

Ocean Redox Structure During the GOE. Shales deposited between 2.32 and 2.1 Ga show the largest and longest-lived positive Se isotope excursion seen in the geologic record (Fig. 2). Several processes other than oxyanion reduction are known to fractionate Se isotopes, but their fractionation factors are too small to explain the shift of $\delta^{82/78}$Se values to >+1‰ (max. + 2.25‰) during the GOE. Oxidative weathering alone is unlikely to generate this magnitude of fractionation relative to crustal values because oxidation generally imparts a small (<0.5‰) fractionation (28). Large fractionations associated with weathering have only been observed in unusually Se-rich soils (up to 2% Se content, ref. 29), whereas Se-lean soils (<0.5 ppm)—more representative of average crust (<0.1 ppm)—show no significant fractionation (±0.25‰, ref. 30). The absence of a significant fractionation during weathering is further supported by isotopic mass balance of marine sediments (26). Assimilation into biomass also causes only small fractionation (<+0.6‰, ref. 31), so changes in biological utilization of Se cannot account for the large excursion. A shift in Se crustal sources cannot explain the heavy isotopic values seen between 2.32 and 2.1 Ga because there is little variability in the Se isotopic composition of different terrestrial reservoirs (crustal source rocks range from −0.3‰ to +0.6‰, ref. 32).

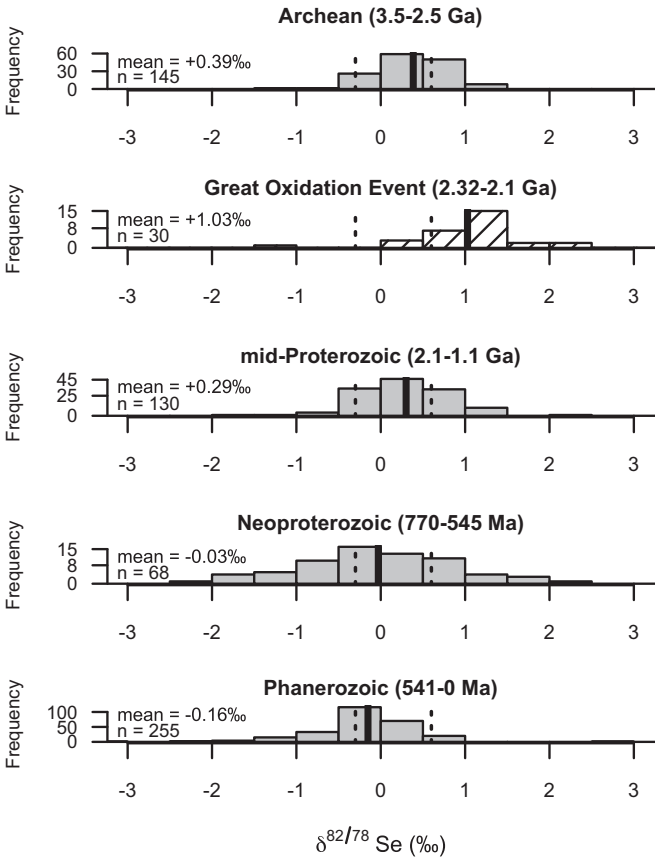

Fig. 3. Histogram of all published shale $\delta^{82/78}$Se values in different stages of geologic time. Dotted lines indicate crustal $\delta^{82/78}$Se range. The interval from ∼2.32–2.1 Ga marks the only time when offshore shales record persistently positive $\delta^{82/78}$Se values. Archean and mid-Proterozoic Se isotope ratios are near crustal values, whereas Neoproterozoic and Phanerozoic values are often negative.

This leaves partial reduction of Se oxyanions as the most likely process to generate large (>1‰) fractionations that can be preserved in sedimentary rocks. In laboratory settings, both biotic and abiotic partial reduction generate isotopic fractionations of several permil, with lighter Se isotopes being preferentially enriched in reduced compounds (33). In bulk samples from natural settings, observed fractionations tend to be smaller (range from −2 to +2‰), perhaps because the isotopic signature of reduced Se gets diluted by codeposition of biologically assimilated Se in sediments (34). Still, dissimilatory reduction can alter the Se isotopic composition of residual oxyanions dissolved in seawater, and this has been documented in the Phanerozoic (35), Neoproterozoic (24), and Archean (36). In the 2.5 Ga Mt. McRae Shale, Se isotopes show a positive excursion parallel with a positive excursion in nitrogen isotopes and enrichments in redox-sensitive trace metals that have been interpreted as evidence for a transient pulse of oxygen that occurred before the onset of the GOE (36–38). Stüeken et al. (36) argued that this Se isotope excursion was generated in a redox-stratified water column where Se was partially reduced in shallow-marine, suboxic waters, driving the residual Se reservoir to more positive $\delta^{82/78}$Se values, which were then recorded in offshore shales. The positive $\delta^{82/78}$Se values seen during the GOE seem to indicate a similar scenario, although in this instance persisting in multiple basins on separate continents over a timescale of hundreds of millions of years.

The fact that most sedimentary Se isotope ratios in Archean and mid-Proterozoic shales do not significantly deviate from crustal values (Fig. 3) suggests that either Se influx was generally low or that Se oxyanions in the oceans during these intervals were quantitatively reduced and assimilated (Fig. 4*A*), allowing sediments to roughly record the isotopic composition of crustal source rocks. The observation of significantly positive $\delta^{82/78}$Se values in all analyzed offshore sediments dating within the GOE thus suggests an extreme isotopic distillation of an expanded marine Se reservoir at this time. To generate such a large isotopic excursion, there were likely extensive near-shore suboxic environments where Se oxyanions were constantly resupplied, allowing substantial nonquantitative reduction to occur in the water column. This would sequester isotopically light Se in near-shore sediments that were not sampled in this study, perhaps with the exception of the Wewe Slate (see below) (Fig. 4*B*). The residual Se reservoir would thus have been driven isotopically heavy. These heavy values could then have been recorded in the offshore environments sampled in this study either by quantitative or nonquantitative reduction and/or biological assimilation, depending on the extent of suboxia on the outer shelf.

This stands in contrast to the modern ocean, which receives a large flux of Se oxyanions but generates only small isotopic fractionations (Fig. 4*C*). Suboxic waters are scarce in the fully oxygenated modern oceans (<10% of ocean area; ref. 39) and diagenetic Se reduction in sediments seems to produce relatively small fractionations, perhaps because the supply of Se oxyanions is diffusion-limited in pore waters. Thus, the magnitude of the positive $\delta^{82/78}$Se excursion seen in shales deposited during the GOE suggests that suboxia was a widespread and persistent feature along continental margins during this interval.

The lack of negative $\delta^{82/78}$Se values in offshore sediments deposited during the GOE also suggests that—unlike in the late Neoproterozoic and Phanerozoic—there was not any resupply of Se oxyanions from an oxic deep-ocean reservoir. This is consistent with previous work that has suggested the deep ocean remained anoxic throughout the GOE (40). So, whereas the Se data alone remain somewhat ambiguous as to the precise redox state of the sampled offshore depositional environments, they can be used to confidently infer the persistence of widespread near-shore suboxia, and predominantly anoxic conditions in the deep ocean.

An isotopic record of Se in near-shore sediments that preserve the complementary negative $\delta^{82/78}$Se values and were deposited coevally with the shales bearing the positive $\delta^{82/78}$Se excursion

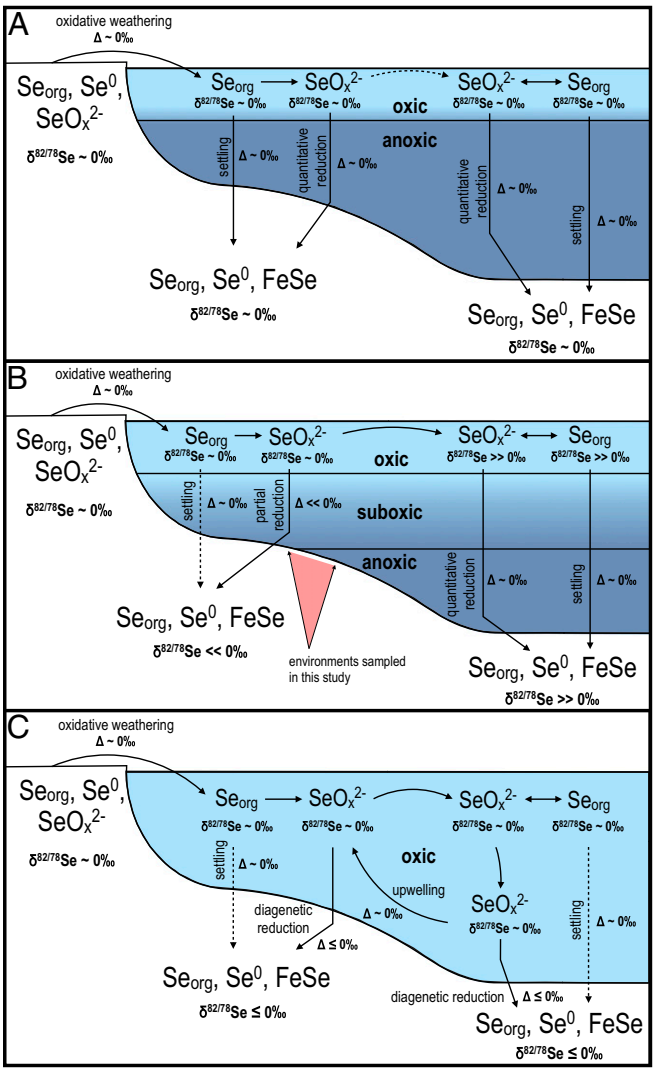

Fig. 4. Sketch of the selenium cycle during (*A*) the late Archean and mid-Proterozoic, (*B*) the Great Oxidation Event, and (*C*) the late Neoproterozoic and Phanerozoic. "$\delta^{82/78}$Se" refers to the isotope ratio of a designated reservoir; "Δ" refers to the isotopic fractionation associated with a designated process. Dotted arrows for Se_{org} burial in oxic/suboxic environments signify that this process has minor significance, but in some cases may dilute sedimentary Se isotope signatures (34). See text for further discussion.

would provide a test of this hypothesis. However, given current sensitivity limits for Se isotope analysis, this remains a challenging prospect. Se concentrations in carbonates, sandstones, and low-TOC shales associated with near-shore depositional environments are orders of magnitude less than in offshore organic-rich shales, requiring unfeasibly large sample sizes to obtain accurate measurements. Further methodological refinement may eventually enable analysis of such materials.

Still, there is some evidence for a complementary light Se reservoir in shallow-water environments during the GOE. The Wewe Slate (~2.2–2.1 Ga) displays by far the largest range of $\delta^{82/78}$Se values of units analyzed in this study (−1.34 to +2.25‰; Dataset S1). We suspect that this is because this unit is capturing the seawater Se composition near the environmental gradient for Se reduction. The Wewe Slate is underlain by mature quartz sandstones and stromatolitic dolostones (41) and has relatively low TSe and TOC contents (Fig. 1, *SI Appendix*), all consistent with a near-shore depositional environment, in contrast to the TSe- and

TOC-rich shales from other units included in this dataset. Because there is no noticeable stratigraphic trend in Se isotopes or abundance through the Wewe Slate (*SI Appendix*), it is unlikely that the range of values reflects secular change in the depositional environment. We cannot rule out the possibility that the Wewe Slate is capturing transient deep-ocean oxygenation in the midst of the GOE, but the sedimentologic context is consistent with deposition of the Wewe Slate in a setting that straddled a chemocline with fluctuating depth, thus sampling both the shallow and deep Se reservoirs.

At the end of the GOE (2.1–2.0 Ga), $\delta^{82/78}$Se values sharply return to crustal values (Fig. 2), consistent with rapid deoxygenation of the ocean (16). The occurrence of some negative $\delta^{82/78}$Se values in the Zaonega and Francevillian formations may result from the weathering of isotopically light Se that was deposited in shallow settings during the GOE, and subsequently uplifted and eroded on tectonic timescales of ∼100 My. However, we cannot definitively rule out the possibility that these data represent a pulse of oxygenation at the culmination of the GOE (11). In either case, the longer-term trend reveals an ultimate return to widespread anoxia. Even if Se influx to the ocean decayed gradually as Se-rich sediments deposited during the GOE were weathered, a contraction of suboxic water masses and takeover by anoxic and strongly euxinic conditions could have rapidly pushed the system toward quantitative reduction of Se oxyanions, thus ending the Se isotopic excursion seen during the GOE. Contraction of the marine Se reservoir during deoxygenation would further accelerate the loss of isotopic fractionation, because a smaller Se reservoir could be quantitatively reduced more easily.

How Oxic Were Near-Shore Environments During the GOE? These data can be used to provide an approximate lower limit on shallow-marine oxygen levels across the GOE. Specifically, when used in conjunction with the iodine record, the Se data point to the presence of conditions that were at least suboxic. In the modern ocean, quantitative reduction of iodate (IO_3^-) to iodide (I^-) has been observed at dissolved O_2 concentrations less than ∼5 μM (42). In the same study, Se oxyanion reduction was nonquantitative at oxygen concentrations down to ∼1 μM O_2. Another investigation of Se speciation in the anoxic Saanich Inlet found that Se oxyanions became depleted to below the detection limit at <0.4 μM O_2 (25). Within this framework, the occurrence of positive $\delta^{82/78}$Se values across the GOE implies a conservative lower limit for shallow-water oxygen concentrations of >0.4 μM O_2. In reality, it is likely that O_2 concentrations were higher in these settings, because reduction of Se oxyanions in near-shore environments was evidently far from being quantitative. High I/(Ca + Mg) ratios in LE-aged carbonates (17) may push the lower limit for surface ocean oxygen up to ∼5 μM O_2 for the later stage of the GOE. This would still only be a small fraction of the modern surface ocean oxygen concentration of ∼325 μM O_2, but it could have had important evolutionary implications.

Implications for Biological Evolution. Whether or not oxygen availability was the primary control on the evolution of deeply rooted eukaryotes remains a highly contentious issue. Recent evidence for extremely low mid-Proterozoic oxygen levels (43) has hinted that low oxygen indeed inhibited the diversification of multicellular, aerobically respiring organisms until the late Neoproterozoic (see ref. 44 for an alternative view). However, the recognition of oxygen-rich conditions in the early Paleoproterozoic opens up the possibility that there was a relatively long (∼200 My) interval that may have been favorable for the evolution of complex life forms long before the fossil record indicates their rise to ecological importance (45, 46).

Convincing fossil evidence of multicellular eukaryotic life is hard to come by in the Proterozoic, but there are numerous reports of fossils purported to have eukaryotic affinity that span nearly the entire temporal extent of the Proterozoic (47–49). These include centimeter-scale structures in the ∼2.1 Ga Francevillian Series of Gabon that have been interpreted as populations of multicellular organisms (50). While such reports remain controversial, a better understanding of the redox architecture of the contemporary oceans would greatly aid our interpretation of the possible affinities of these ambiguous fossilized life forms.

The observed lower limit for survival of aerobically respiring benthic animals is ∼0.88 μM O_2 (51, 52), and theoretical considerations suggest that the actual limit is even lower (53). For steroid synthesis in unicellular eukaryotes, a lower limit of 7 nM O_2 has been inferred (54) and aerobic respiration in bacteria continues down to 3 nM (55). The lower limit proposed here of >0.4 μM O_2 in near-shore environments during the GOE therefore suggests that O_2 levels were high enough for the existence of eukaryotic organisms in multiple basins over a long period. However, these limits are very close to the metazoan O_2 threshold and so it is quite possible (and perhaps likely) that the evolution of motile, multicellular eukaryotes was hindered by redox instability at this time (20, 56). Nonetheless, the existing data allow the possibility that the early phases of unicellular eukaryotic evolution could have been underway in the early Paleoproterozoic. Subsequently lowered oxygen levels may have delayed the eukaryotic rise to ecological abundance for more than a billion years. Without a more complete fossil record it is all but impossible to test whether this was indeed the case. Nevertheless, during the GOE the redox restriction on microbial aerobic metabolism could have been lifted over wide areas of the continental shelves for the first time in Earth's history.

Conclusions

An increase in the abundance of Se in organic-rich shales deposited during the GOE is consistent with enhanced oxidative continental weathering at this time, and corroborates evidence from other redox-sensitive proxies (S, Mo, and U). A shift to the most positive offshore $\delta^{82/78}$Se values in geologic history suggests that extensive partial reduction of Se oxyanions in shallow, suboxic seawater drove the isotopic composition of residual oceanic Se heavier. Shallow-marine sediments thus acted as a sink for isotopically light Se, perhaps recorded by the negative $\delta^{82/78}$Se ratios found in the Wewe Slate. This state of enhanced oxidative continental weathering and extensive shallow-ocean suboxia appears to have prevailed until near the end of the GOE, when plummeting Se/TOC ratios and $\delta^{82/78}$Se values suggest that the marine Se reservoir rapidly diminished and suboxic water masses contracted at the expense of anoxic and, possibly, strongly euxinic waters. Thus, the period from ∼2.32–2.1 Ga was the first interval in Earth's history when conditions that were at least suboxic persisted on continental margins on geological timescales, perhaps supporting the early evolution of aerobically respiring life forms. The contraction of oxic and suboxic environments after the GOE may have limited the available habitats for the evolutionary radiation of eukaryotic life until the second rise of oxygen in the late Neoproterozoic.

Methods

Samples were prepared and analyzed following the methods of Stüeken et al. (57). Rock powders were dissolved using HF, HNO_3, and $HClO_4$, and Se was isolated using thiol-cotton fiber columns. All analyses were conducted on a hydride-generator multicollector inductively coupled plasma mass spectrometer (Nu Instruments). Measurements were normalized using standard-sample bracketing. We note that both $\delta^{82/76}$Se and $\delta^{82/78}$Se notations are used in the literature; our data are expressed as $\delta^{82/78}$Se relative to National Institute of Standards and Technology reference SRM 3149 because, using our isotopic measurement method, mass 78 is much less affected by isobaric interferences than mass 76 (57). Average precision (1σ) for samples was 0.067‰ for $\delta^{82/78}$Se values and 0.022 ppm for Se concentrations. $\delta^{82/78}$Se values for international reference material SGR-1 and in-house standard

UW-McRae were +0.12 ± 0.18‰ (1σ, $n = 5$) and +0.85 ± 0.18‰ (1σ, $n = 27$), respectively, which agree well with published values (22, 23).

TOC analysis followed Stüeken (58). Carbonate was removed from rock powders via acidification with HCl. Decarbonated powders were analyzed on a Costech ECS 4010 Elemental Analyzer coupled to a continuous flow isotope-ratio mass spectrometer (Finnigan MAT253) via a ThermoFinnigan Conflo III. Average precision for TOC measurements was 0.17% (1σ, $n = 49$).

ACKNOWLEDGMENTS. We thank Aivo Lepland, Chris Reinhard, Pavel Medvedev, Luke Ootes, Frantz Ossa-Ossa, New Millennium Iron, Cliffs Natural Resources, and the Geological Survey of Botswana for access to samples critical to this work. We thank the University of Washington Isotope Geochemistry Lab for technical support. Funding for this work was provided by National Science Foundation (NSF) Grant EAR-0921580, NSF Frontiers in Earth System Dynamics Grant 1338810, and NASA Grant NNX16AI37G to R.B., as well as NSF Grant EAR-05-45484, NASA Astrobiology Institute Award NNA04CC09A, and an Natural Sciences and Engineering Research Council of Canada Discovery and Accelerator Grant (to A.B.). M.A.K. acknowledges support from an NSF Graduate Research Fellowship. E.E.S. is supported by a NASA Postdoctoral Fellowship. Additional support was provided by the NASA Astrobiology Institute Virtual Planetary Laboratory team Grant NNA13AA93A.

1. Holland HD (1984) *The Chemical Evolution of the Atmosphere and Oceans* (Princeton Univ Press, Princeton).
2. Lyons TW, Reinhard CT, Planavsky NJ (2014) The rise of oxygen in Earth's early ocean and atmosphere. *Nature* 506(7488):307–315.
3. Bekker A, Holland HD (2012) Oxygen overshoot and recovery during the early Paleoproterozoic. *Earth Planet Sci Lett* 317:295–304.
4. Schidlowski M, Trurnit P (1966) Drucklösungserscheinungen an Geröllpyriten aus den Witwatersrand-Konglomeraten. Ein Beitrag zur Frage des diagenetischen Verhaltens von Sulfiden. *Schweiz Mineral Petrogr Mitt* 46:332–342.
5. Rasmussen B, Buick R (1999) Redox state of the Archean atmosphere: Evidence from detrital heavy minerals in ca. 3250–2750 Ma sandstones from the Pilbara Craton, Australia. *Geology* 27(2):115–118.
6. Cloud PE, Jr (1968) Atmospheric and hydrospheric evolution on the primitive earth. Both secular accretion and biological and geochemical processes have affected earth's volatile envelope. *Science* 160(3829):729–736.
7. Farquhar J, Bao H, Thiemens M (2000) Atmospheric influence of Earth's earliest sulfur cycle. *Science* 289(5480):756–759.
8. Pavlov AA, Kasting JF (2002) Mass-independent fractionation of sulfur isotopes in Archean sediments: Strong evidence for an anoxic Archean atmosphere. *Astrobiology* 2(1):27–41.
9. Bekker A, et al. (2004) Dating the rise of atmospheric oxygen. *Nature* 427(6970): 117–120.
10. Luo G, et al. (2016) Rapid oxygenation of Earth's atmosphere 2.33 billion years ago. *Sci Adv* 2(5):e1600134.
11. Kump LR, et al. (2011) Isotopic evidence for massive oxidation of organic matter following the great oxidation event. *Science* 334(6063):1694–1696.
12. Bekker A (2015) Lomagundi carbon isotope excursion, *Encyclopedia of Astrobiology*, eds Gargaud M, et al. (Springer, Berlin), 2nd Ed, p 1–6.
13. Karhu JA, Holland HD (1996) Carbon isotopes and the rise of atmospheric oxygen. *Geology* 24(10):867–870.
14. Schröder S, Bekker A, Beukes NJ, Strauss H, Van Niekerk HS (2008) Rise in seawater sulphate concentration associated with the Paleoproterozoic positive carbon isotope excursion: Evidence from sulphate evaporites in the 2.2–2.1 Gyr shallow-marine Lucknow Formation, South Africa. *Terra Nova* 20(2):108–117.
15. Planavsky NJ, Bekker A, Hofmann A, Owens JD, Lyons TW (2012) Sulfur record of rising and falling marine oxygen and sulfate levels during the Lomagundi event. *Proc Natl Acad Sci USA* 109(45):18300–18305.
16. Scott C, et al. (2014) Pyrite multiple-sulfur isotope evidence for rapid expansion and contraction of the early Paleoproterozoic seawater sulfate reservoir. *Earth Planet Sci Lett* 389:95–104.
17. Hardisty DS, et al. (2014) An iodine record of Paleoproterozoic surface ocean oxygenation. *Geology* 42(7):619–622.
18. Scott C, et al. (2008) Tracing the stepwise oxygenation of the Proterozoic ocean. *Nature* 452(7186):456–459.
19. Partin CA, et al. (2013) Large-scale fluctuations in Precambrian atmospheric and oceanic oxygen levels from the record of U in shales. *Earth Planet Sci Lett* 369: 284–293.
20. Reinhard CT, Planavsky NJ, Olson SL, Lyons TW, Erwin DH (2016) Earth's oxygen cycle and the evolution of animal life. *Proc Natl Acad Sci USA* 113(32):8933–8938.
21. Canfield DE, et al. (2013) Oxygen dynamics in the aftermath of the Great Oxidation of Earth's atmosphere. *Proc Natl Acad Sci USA* 110(42):16736–16741.
22. Mitchell K, et al. (2012) Selenium as paleo-oceanographic proxy: A first assessment. *Geochim Cosmochim Acta* 89:302–317.
23. Stüeken EE, et al. (2015) The evolution of the global selenium cycle: Secular trends in Se isotopes and abundances. *Geochim Cosmochim Acta* 162:109–125.
24. von Strandmann PAP, et al. (2015) Selenium isotope evidence for progressive oxidation of the Neoproterozoic biosphere. *Nat Commun* 6:10157.
25. Cutter GA (1982) Selenium in reducing waters. *Science* 217(4562):829–831.
26. Stüeken EE (2017) Selenium isotopes as a biogeochemical proxy. *Rev Mineral Geochem* 82:657–682.
27. Stüeken EE, Catling DC, Buick R (2012) Contributions to late Archaean sulphur cycling by life on land. *Nat Geosci* 5(10):722–725.
28. Johnson TM (2004) A review of mass-dependent fractionation of selenium isotopes and implications for other heavy stable isotopes. *Chem Geol* 204(3):201–214.
29. Zhu J-M, Johnson TM, Clark SK, Zhu X-K, Wang X-L (2014) Selenium redox cycling during weathering of Se-rich shales: A selenium isotope study. *Geochim Cosmochim Acta* 126:228–249.
30. Schilling K, Johnson TM, Wilcke W (2011) Selenium partitioning and stable isotope ratios in urban topsoils. *Soil Sci Soc Am J* 75(4):1354–1364.
31. Clark SK, Johnson TM (2010) Selenium stable isotope investigation into selenium biogeochemical cycling in a lacustrine environment: Sweitzer Lake, Colorado. *J Environ Qual* 39(6):2200–2210.
32. Rouxel O, Ludden J, Carignan J, Marin L, Fouquet Y (2002) Natural variations of Se isotopic composition determined by hydride generation multiple collector inductively coupled plasma mass spectrometry. *Geochim Cosmochim Acta* 66(18):3191–3199.
33. Johnson TM, Bullen TD (2004) Mass-dependent fractionation of selenium and chromium isotopes in low-temperature environments. *Rev Mineral Geochem* 55(1): 289–317.
34. Mitchell K, Mansoor SZ, Mason PRD, Johnson TM, Van Cappellen P (2016) Geological evolution of the marine selenium cycle: Insights from the bulk shale δ82/76Se record and isotope mass balance modeling. *Earth Planet Sci Lett* 441:178–187.
35. Wen H, et al. (2014) Selenium isotopes trace anoxic and ferruginous seawater conditions in the Early Cambrian. *Chem Geol* 390:164–172.
36. Stüeken EE, Buick R, Anbar AD (2015) Selenium isotopes support free O-2 in the latest Archean. *Geology* 43(3):259–262.
37. Anbar AD, et al. (2007) A whiff of oxygen before the great oxidation event? *Science* 317(5846):1903–1906.
38. Garvin J, Buick R, Anbar AD, Arnold GL, Kaufman AJ (2009) Isotopic evidence for an aerobic nitrogen cycle in the latest Archean. *Science* 323(5917):1045–1048.
39. Paulmier A, Ruiz-Pino D (2009) Oxygen minimum zones (OMZs) in the modern ocean. *Prog Oceanogr* 80(3):113–128.
40. Bekker A, et al. (2008) Fractionation between inorganic and organic carbon during the Lomagundi (2.22–2.1 Ga) carbon isotope excursion. *Earth Planet Sci Lett* 271(1): 278–291.
41. Bekker A, Karhu JA, Kaufman AJ (2006) Carbon isotope record for the onset of the Lomagundi carbon isotope excursion in the Great Lakes area, North America. *Precambrian Res* 148(1):145–180.
42. Rue EL, Smith GJ, Cutter GA, Bruland KW (1997) The response of trace element redox couples to suboxic conditions in the water column. *Deep Sea Res Part I* 44(1):113–134.
43. Planavsky NJ, et al. (2014) Earth history. Low mid-Proterozoic atmospheric oxygen levels and the delayed rise of animals. *Science* 346(6209):635–638.
44. Zhang S, et al. (2016) Sufficient oxygen for animal respiration 1,400 million years ago. *Proc Natl Acad Sci USA* 113(7):1731–1736.
45. Knoll AH (2011) The multiple origins of complex multicellularity. *Annu Rev Earth Planet Sci* 39:217–239.
46. Narbonne GM (2005) The ediacarabiota: Neoproterozoic origin of animals and their ecosystems. *Annu Rev Earth Planet Sci* 33:421–442.
47. Walter MR, Oehler JH, Oehler DZ (1976) Megascopic algae 1300 million years old from the Belt Supergroup, Montana: A reinterpretation of Walcott's Helminthoidichnites. *J Paleontol* 50(5):872–881.
48. Sharma M, Shukla Y (2009) Taxonomy and affinity of Early Mesoproterozoic megascopic helically coiled and related fossils from the Rohtas Formation, the Vindhyan Supergroup, India. *Precambrian Res* 173(1):105–122.
49. Zhu S, et al. (2016) Decimetre-scale multicellular eukaryotes from the 1.56-billion-year-old Gaoyuzhuang Formation in North China. *Nat Commun* 7:11500.
50. El Albani A, et al. (2010) Large colonial organisms with coordinated growth in oxygenated environments 2.1 Gyr ago. *Nature* 466(7302):100–104.
51. Levin L, et al. (2002) Benthic processes on the Peru margin: A transect across the oxygen minimum zone during the 1997–98 El Niño. *Prog Oceanogr* 53(1):1–27.
52. Breuer ER, et al. (2009) Sedimentary oxygen consumption and microdistribution at sites across the Arabian Sea oxygen minimum zone (Pakistan margin). *Deep Sea Res Part II Top Stud Oceanogr* 56(6):296–304.
53. Sperling EA, Halverson GP, Knoll AH, Macdonald FA, Johnston DT (2013) A basin redox transect at the dawn of animal life. *Earth Planet Sci Lett* 371:143–155.
54. Waldbauer JR, Newman DK, Summons RE (2011) Microaerobic steroid biosynthesis and the molecular fossil record of Archean life. *Proc Natl Acad Sci USA* 108(33): 13409–13414.
55. Stolper DA, Revsbech NP, Canfield DE (2010) Aerobic growth at nanomolar oxygen concentrations. *Proc Natl Acad Sci USA* 107(44):18755–18760.
56. Johnston DT, et al. (2012) Late Ediacaran redox stability and metazoan evolution. *Earth Planet Sci Lett* 335:25–35.
57. Stüeken EE, Foriel J, Nelson BK, Buick R, Catling DC (2013) Selenium isotope analysis of organic-rich shales: Advances in sample preparation and isobaric interference correction. *J Anal At Spectrom* 28(11):1734–1749.
58. Stüeken EE (2013) A test of the nitrogen-limitation hypothesis for retarded eukaryote radiation: Nitrogen isotopes across a Mesoproterozoic basinal profile. *Geochim Cosmochim Acta* 120:121–139.